# Structure and Dynamics of the Compression Induced Polycrystalline-Glass Transition

# CNF Summer Student: Sylvie Shaya Student Affiliation: Wellesley College Department of Physics

Summer Program(s): 2025 Cornell NanoScale Facility Research Experience for Undergraduates (CNF REU) Program, SUPREME REU

Principal Investigator(s): Julia Dshemuchadse, Erin Teich

Mentor(s): Katherine Wang

Primary Source(s) of Research Funding: National Science Foundation award NNCI- 2025233 Contact: jd732@cornell.edu, et106@wellesley.edu, xw682@cornell.edu, ss131@wellesley.edu

Summer Program Website(s): https://cnf.cornell.edu/education/reu Research Group Website: https://capecrystal.mse.cornell.edu/

### **Abstract:**

When polycrystal grain size is sufficiently reduced, materials undergo a solid-to-glass transition that is distinct from the more commonly studied liquid-to-glass transition and is critical to understanding the behavior of ultrafine-grained polycrystals. These materials hold promise in microelectronics and thermoelectrics, yet their behavior at and beyond the glass transition is not well understood. We simulate a binary system of hard and soft particles under compression to investigate the structure and dynamics of the polycrystalline-to-glass transition. Our results reveal a strong relationship between local structural features and dynamical behavior and indicate that soft particles play an outsized role in the glass transition, as they are associated with areas of strong dynamics and disorder.

## **Summary of Research:**

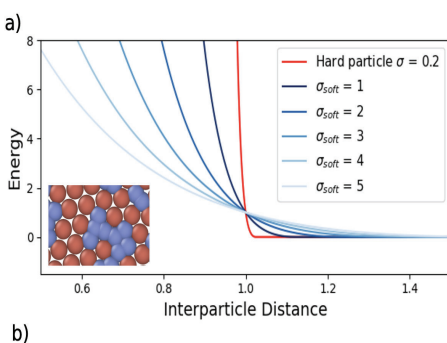
#### **Background:**

Polycrystals are known to exhibit Hall–Petch behavior, which describes how materials strengthen as grain size is reduced. As grain size is further decreased and grain boundary behavior dominates, polycrystals soften and become glassy [1]. Ultrafine-grained polycrystals display properties of interest for materials applications, including high electrical conductivity and reduced thermal conductivity, and understanding the polycrystalline-to-glass transition is critical for further development of these materials [2].

#### Simulation Methods:

We perform molecular dynamics simulations on a binary system of 6400 hard and 6400 soft discs using the simulation toolkit HOOMD-blue [3]. Particle interactions were defined by Weeks—Chandler—Andersen potentials shifted radially to ensure all particles have the same effective diameter of d=1, with Lorentz—Berthelot mixing rules applied to cross-interactions, described in Fig. 1(b). Particle softness was denied via  $\sigma$ , which varies the shape of the potential well. Hard-particle softness was defined as  $\sigma=0.2$  and held constant for all systems, and soft- particle softness was varied between

 $\sigma_{\text{soft}} = 1$  and 5, as shown in Fig. 1(a).



$$U(r) = \begin{cases} 4\epsilon((\frac{\sigma}{r - \Delta})^{12} - (\frac{\sigma}{r - \Delta})^{6}) - \epsilon & r < 2^{1/6}\sigma + \Delta \\ 0 & r \ge 2^{1/6}\sigma + \Delta \end{cases}$$
 (1)

$$\Delta = \frac{(d_{hard} + d_{soft})}{2} - \sigma \tag{2}$$

$$\sigma_{ij} = \frac{\sigma_{ii} + \sigma_{jj}}{2}$$
  $\epsilon_{ij} = (\epsilon_{ii}\epsilon_{jj})^{1/2}$  (3)

Figure 1: Model setup. (a) Particle interactions via Weeks—Chandler—Andersen potentials for various softnesses  $\sigma$ . (b) Equations describing particle interactions. 1.) Weeks—Chandler—Andersen potentials, shifted radially by a factor  $\Delta$ , defined in equation 2.). 3.) Lorentz—Berthelot mixing rules.

The system was initialized at low density, then randomized and compressed to a density between  $\phi = 0.8$  and  $\phi = 1.1$ . Following compression, the system was equilibrated to account for artifacts from the compression step, then run for  $10^8$  molecular dynamics timesteps to collect data. Simulation temperature was fixed at kT = 0.2.

#### Results:

To establish the system's glassiness, we investigate the mean squared displacement (MSD) and the non-Gaussian parameter  $\alpha(t)$ , an indicator of dynamical heterogeneity. Glassy systems feature a plateau in MSD and a peak in  $\alpha(t)$  at intermediate time scales, due to particles being trapped in cages of their neighbors before moving collectively at long time scales [4]. At low  $\sigma_{soft}$ , the system is crystalline and shows neither of

these features. We chose to focus on  $\sigma$ soft = 4, where we observe these behaviors at  $\phi$ -values above 0.9, indicating that the system is glassy.

The compression of the system can be seen in the radial distribution functions (RDFs), where hard–soft and soft–soft RDF peaks are broader and located at smaller distances r than hard–hard peaks, seen in Fig. 2(a), as soft particles overlap under compression. There are clear peaks in the RDF at low  $\phi$ , which disappear under compression, as shown in Fig. 2(b), reflecting the existence and subsequent breakdown of long-range order as the system transitions into a glass.

Lattice structure was characterized through the hexatic order parameter  $\psi_6$ . Global  $\psi_6$  is maximal (at 1) when the system is crystalline, and decreases at higher  $\phi$ , shown in Fig. 2(c). At high densities, the distribution of soft particle  $\psi_6$  is flatter than that of hard particles, seen in Fig. 2(d), indicating that soft particles tend to be more disordered than hard particles.

To characterize the dynamics of the system, we calculate the Lindemann parameter L, a measure of the strength of particle dynamics, and  $D^2$ min, an indicator of irreversible rearrangements [1, 5]. At low densities, particles with large L and D2min exist primarily along grain boundaries. As density increases, high L and  $D^2$ min particles form clusters throughout the system, as seen in Figs. 3(a)-(b). The distribution of soft-particle Ls and  $D^2$ min is higher than those of hard particles, seen in Figs. 3(d)-(e), indicating that soft particles display stronger dynamics than hard particles.

To understand the relationship between dynamical parameters and structure, we calculated the covariances of D2min with the number of soft neighbor particles and L with  $\psi_6$ , shown in Fig. 4(a)-(b). For  $\sigma_{soft} = 4$ , there is a peak at  $\phi = 0.9$  for both covariances. The peak of the covariance of L and  $\psi^6$  has been shown to correlate to the polycrystalline-to-glass transition [1]. We observe a peak in the same location in the covariance of D²min and number of soft neighbors, in Fig. 4(b), demonstrating a clear relationship between structure and dynamics at the glass transition.

As  $\sigma_{soft}$  increases, the peak of the covariance, and in turn the glass transition, shifts lower in density, seen in Fig 4(b). The global average  $\psi_6$  shifts similarly, as seen in Fig. 2(c), as the breakdown in structure associated with the glass transition shifts.

### **Conclusion and Future Steps:**

Under compression, binary systems of hard and soft particles display interesting behavior as they undergo a polycrystalline-to-glass transition. There is a strong relationship between the structure and dynamics of the system, seen in the covariances of dynamical and structural properties. Soft- particle softness impacts the location of the glass transition in density space, and soft particles appear to play an outsized role in this transition, as they tend to have stronger dynamics and disorder than hard particles.

Future steps include improved characterization of the

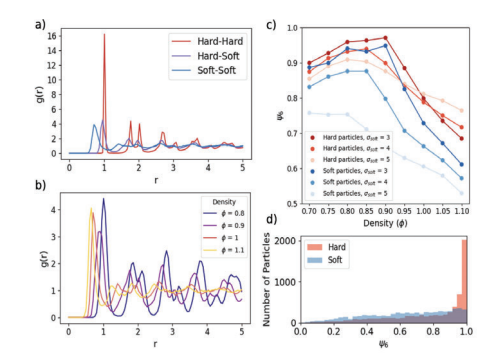


Figure 2: Structural parameters. (a) Type-wise RDFs for the 100th frame of simulations with  $\sigma_{soft} = 4$  and  $\phi = 1$ . (b) Soft-soft RDFs for  $\sigma_{soft} = 4$  over various  $\phi$  values. (c) Global average  $\psi_6$  for hard and soft particles. (d) Distributions of  $\psi$ 6 by particle type at the 100th frame of simulations with  $\sigma$ soft = 4 and  $\phi$  = 1.

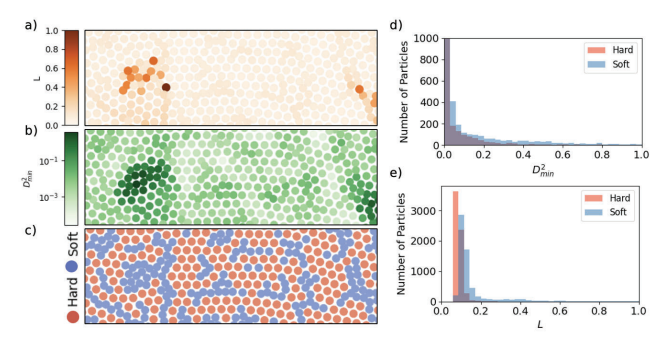


Figure 3: Dynamical characterizations, calculated over the first 100 frames of simulations with  $\sigma_{soft} = 4$  and  $\phi = 1$ . (a) Heatmap of L. (b) Heatmap of  $D^2_{min}$  with a logarithmic colormap. (c) Particle identities at the 100th frame of simulation. (d) Histogram of L by particle type. (e) Histogram of  $D^2_{min}$  by particle type.

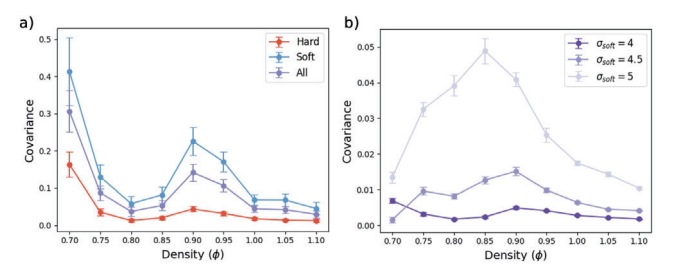


Figure 4: Covariances of dynamics and structure. (a) Typewise covariances of  $D^2_{min}$  and number of soft particle neighbors for  $\sigma_{soft} = 4$ . (b) All particle covariances of disorder, defined as  $1 - \psi_{\theta}$  and L over various  $\sigma$ soft values.

relationship between structure and dynamics through statistical analysis, and descriptions of the collective motion of particles. Qualitative observation of the system indicates the existence of string- and loop-like cooperative motion, which in future work could be related to the structure of the system.

#### **References:**

- [1] Zhang, H. & Han, Y. Physical Review X 8, 041023 (2018).
- [2] Lu, L. et al. Science 304, 422–426 (2004).
- [3] Anderson, J.A. et al. Computational Materials Science 173, 109363 (2020).
- [4] Teich, E.G. et al. Nature Communications 10, 64 (2019).
- [5] Falk, M.L. & Langer, J.S. Physical Review E 57, 7192 (1998).